Inorganic Chemistry

ARTICLE

pubs.acs.org/IC

Ratiometric Phosphorescence Imaging of Hg(II) in Living Cells Based on a Neutral Iridium(III) Complex

Yongquan Wu,[†] Hao Jing,[†] Zesheng Dong,[†] Qiang Zhao,*[,‡] Huazhou Wu,[†] and Fuyou Li*[,†]

[†]Department of Chemistry, Fudan University, Shanghai, 200433, P. R. China

[‡]Key Laboratory for Organic Electronics & Information Displays (KLOEID) and Institute of Advanced Materials (IAM), Nanjing University of Posts and Telecommunications, Nanjing 210046, P. R. China

Supporting Information

ABSTRACT: In this work, a neutral iridium(III) complex $[Ir(bt)_2(acac)]$ (Hbt = 2-phenylbenzothiazole; Hacac = acetylacetone) has been realized as a Hg(II)-selective sensor through UV−vis absorption, phosphorescence emission, and electrochemical measurements and was further developed as a phosphorescent agent for monitoring intracellular Hg(II). Upon addition of Hg(II) to a solution of $[Ir(bt)_2(acac)]$, a noticeable spectral blue shift in both absorption and phosphorescent emission bands was measured. ^{1}H NMR spectroscopic titration experiments indicated that coordination of Hg(II) to the complex induces fast decomposition of $[Ir(bt)_2(acac)]$ to form a new complex, which is responsible for the significant variations in optical and electrochemical signals. Importantly, cell imaging experiments have shown that $[Ir(bt)_2(acac)]$ is membrane permeable and can be used to monitor the changes in Hg(II) levels within cells in a ratiometric phosphorescence mode.

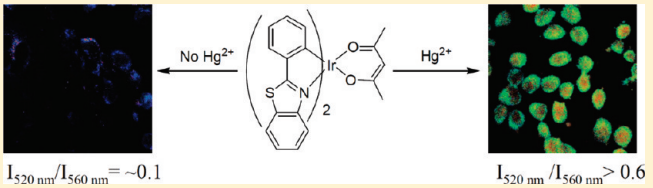

INTRODUCTION

Cyclometalized iridium(III) complexes that possess a d^6-electron configuration show strong spin−orbit coupling, efficient intersystem crossing from the singlet excited state to the triplet manifold, as well as an enhancement of the T_1−S_0 transition, thereby displaying efficient phosphorescent emission at room temperature.[1,2] Due to their rich excited states, these iridium(III) complexes show unique photophysical properties, such as significant Stokes shifts for easy separation of excitation and emission and relatively long lifetimes compared to purely organic luminophores for eliminating fluorescent backgrounds by time-gated technology.[3] Therefore, in recent years, phosphorescent iridium(III) complexes have been applied in the fields of chemosensors,[4−6] biolabeling, and bioimaging.[7−9] For example, Lo's group and our group independently reported approximately 50 phosphorescent iridium(III) complexes suitable for cellular imaging; some of these are capable of staining compartments within living cells.[8−10] The effects of charge and lipophilicity on the celluar uptake of the iridium complexes were investigated in detail. Since positively charged compounds can generally traverse cell membranes more easily, this prior research focused exclusively on cationic iridium complexes. In addition, most of the reported chemosensors based on iridium(III) complexes can detect analytes in solution but not in biological samples.

Combinations of the recognition properties of chemosensors and the monitoring capability of bioimaging based on phosphorescent iridium(III) complexes have rarely been reported. To date, there has been only one example of such of phosphorescent cationic iridium(III) complexes to monitor cysteine/homocysteine in living cells reported by us.[10] We are interested in developing the potential application of neutral phosphorescent iridium(III) complexes for cell imaging and intracellular detection. In the work described herein, we synthesized a neutral phosphorescent iridium(III) complex $[Ir(bt)_2(acac)]$ (**Ir-1**, Hbt = 2-phenylbenzothiazole, Hacac = acetylacetone, Scheme 1) containing sulfur atoms and found that it can enter the living cells and monitor intracellular Hg(II). The photophysical and electrochemical properties of **Ir-1** have been investigated in the absence and presence of Hg(II) ions, and the complex showed an obvious blue shift in its absorption and emission spectra upon addition of Hg(II). Furthermore, internalization of **Ir-1** into the living cells was investigated, and monitoring intracellular Hg(II) has been achieved with ratiometric luminescence bioimaging. For comparison, two other cationic iridium(III) complex salts, $[Ir(bt)(bpy)]PF_6$ (**Ir-2**, bpy = bipyridine) and $[Ir(bt)_2(CH_3CN)_2]OTf$ (**Ir-3**, OTf = trifluoromethanesulfonate) (Scheme 1), have also been studied to compare their sensing ability.

EXPERIMENTAL SECTION

Materials. 2-Phenylbenzothiazole (bt), bipyridine (bpy), silver trifluoromethanesulfonate (AgOTf), tetrabutylammonium hexafluorophosphate (Bu_4NPF_6), KPF_6, 3-(4,5-dimethylthiazol-2-yl)-2,5-diphenyltetrazolium bromide (MTT), and acetylacetone (Hacac) were purchased from Acros. $IrCl_3 \cdot 3H_2O$ (Ir content > 54.51%) was an industrial product and used without further purification. $Hg(ClO_4)_2 \cdot 3H_2O$,

Received: October 14, 2010
Published: July 20, 2011

Scheme 1. Chemical Structures of $[Ir(bt)_2(acac)]$ (Ir-1), $[Ir(bt)_2(bpy)]PF_6$ (Ir-2), and $[Ir(bt)_2(CH_3CN)_2]OTf$ (Ir-3)

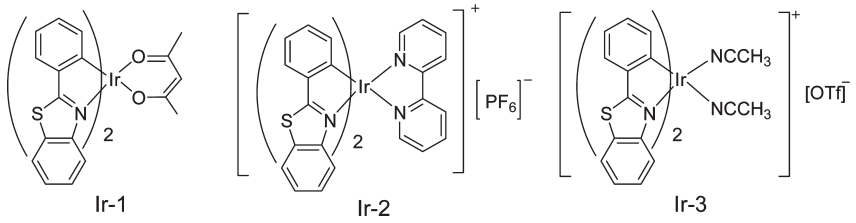

$Pb(NO_3)_2$, $Mg(NO_3)_2$, $Zn(NO_3)_2 \cdot 6H_2O$, $Ni(NO_3)_2 \cdot 6H_2O$, KNO_3, $NaNO_3$, $Co(NO_3)_2 \cdot 6H_2O$, $Cd(NO_3)_3$, $Cr(NO_3)_3 \cdot 9H_2O$, $Cu(NO_3)_2 \cdot 3H_2O$, $FeSO_4 \cdot 7H_2O$, $CuSO_4$, and other reagents were purchased from Sinopharm Chemical Reagent Co., Ltd. (Shanghai, China).

General Experiments. ^1H NMR spectra were recorded with a Varian spectrometer at 400 MHz. Electrospray ionization mass spectra (ESI-MS) were measured on a Micromass LCTTM system. The UV−vis spectra were recorded on a Shimadzu UV-2550 spectrometer. Steady-state emission experiments at room temperature were measured on an Edinburgh Instruments spectrometer. The luminescence quantum yields of iridium complexes in air-equilibrated solution were measured with reference to quinine sulfate as a standard (yield = 0.53, in 0.1 M H_2SO_4, λ_{ex} = 365 nm). Electrochemical measurements were performed with an Eco Chemie Autolab. All measurements were carried out in a one-compartment cell under N_2 gas, equipped with a glassy-carbon working electrode, a platinum wire counter electrode, and a Ag/Ag^+ reference electrode. The supported electrolyte was a 0.10 mol L^{-1} CH_3CN solution of tetrabutylammonium hexafluorophosphate (Bu_4NPF_6). The ferrocene/ferrocenium couple was added and used as the internal standard. The scan rate was 100 $mV \cdot s^{-1}$.

Synthesis of $[Ir(bt)_2(acac)]$ (Ir-1). Complex **Ir-1** was synthesized according to previous literature.[11] A mixture of 2-ethoxyethanol and water (3:1, v/v) was added to a flask containing $IrCl_3 \cdot 3H_2O$ (1 mmol) and phenylbenzothiazole (2.2 mmol). The mixture was heated under reflux for 24 h. After cooling to room temperature, the red solid precipitate was filtered to give crude cyclometalated iridium(III) chloro-bridged dimer $[Ir_2(bt)_4Cl_2]$ (0.2 mmol) and K_2CO_3 (1.4 mmol) were added 2-ethoxyethanol and Hacac (0.5 mmol), and then the slurry was refluxed for 12 h. After cooling to room temperature, a brown-red precipitate was collected by filtration and chromatographed using CH_2Cl_2/petroleum ether (3:2, v/v) to give **Ir-1**, red solid. Yield: 45%; mp 269−270 °C. ^1H NMR ($CDCl_3$, 400 MHz): δ (ppm) 8.09 (d, J = 5.6 Hz, 2H), 7.92 (d, J = 8.0 Hz, 2H), 7.68 (t, J = 7.6 Hz, 2H), 7.45 (d, J = 7.4 Hz, 2H), 7.24 (t, J = 5.8 Hz, 2H), 6.81 (t, J = 7.0 Hz, 2H), 6.68 (t, J = 7.0 Hz, 2H), 6.31 (d, J = 8.0 Hz, 2H), 5.13 (s, 1H), 1.78 (s, 6H). Anal. Calcd for $C_{31}H_{23}IrN_2O_2S_2$: C, 52.30; H, 3.26; N, 3.94. Found: C, 52.08; H, 3.30; N, 3.47. ESI-MS: m/z 712.1(M^+).

Synthesis of $[Ir(bt)_2(bpy)]PF_6$ (Ir-2). A mixture of cyclometalated iridium(III) chloro-bridged dimer $[Ir_2(bt)_4Cl_2]$ (120 mg, 0.1 mmol) and bipyridine (37 mg, 0.24 mmol) in 30 mL of CH_2Cl_2/MeOH (1:1 v/v) was heated at reflux under nitrogen for 6 h. The solution was then cooled to room temperature, and KPF_6 (0.24 mmol) was added to the solution. Then, the mixture was evaporated under reduced pressure. Lastly, chromatography on silica gel with CH_2Cl_2/acetone (4:1, v/v, R_f = 0.37) as the eluent gave 0.10 g (yield 56%) of **Ir-2** as a yellow solid. ^1H NMR (400 MHz, $CDCl_3$): δ (ppm) 8.57 (d, J = 8.4 Hz, 2H), 8.16 (t, J = 7.6 Hz, 2H), 8.07 (d, J = 5.2 Hz, 2H), 7.85 (d, J = 8.0 Hz, 2H), 7.80 (d, J = 7.2 Hz, 2H), 7.50 (t, J = 6.4 Hz, 2H), 7.33 (t, J = 8.0 Hz, 2H), 7.07 (m, 4H), 6.85 (t, J = 7.2 Hz, 2H), 6.38 (d, J = 7.6 Hz, 2H), 6.10 (d, J = 8.4 Hz, 2H). Anal. Calcd for $C_{36}H_{24}IrF_6N_4PS_2$: C, 47.31; H, 2.65; N, 6.13. Found: C, 47.55; H, 3.01; N, 5.80. ESI-MS: m/z 769.1 ($[M - PF_6]^+$).

Synthesis of $[Ir(bt)_2(CH_3CN)_2]OTf$ (Ir-3). $[Ir_2(bt)_4Cl_2]$ (120 mg, 0.1 mmol) and AgOTf (62 mg, 0.24 mmol) were placed in a flask. Acetonitrile (15 mL) and dichloromethane (15 mL) were added, and the slurry was stirred at room temperature for 6 h. The solution was filtered, and the precipitate was washed three times with CH_3CN (0.5 mL × 3). The filtrate and washings were combined and reduced by evaporation to a volume of 1 mL. The solution was cooled to −10 °C, and ether (15 mL) was slowly added while stirring. The yellow precipitate which formed was collected by filtration, washed with ether, and dried under vacuum for 24 h to yield the product. The product is a yellow solid (0.12 g, 70% yield). ^1H NMR ($CDCl_3$), δ (ppm): 8.45 (d, J = 8.4 Hz, 2H), 8.01 (d, J = 8.0 Hz, 2H), 7.78 (t, J = 5.8 Hz, 2H), 7.62 (t, J = 8.0 Hz, 4H), 6.93 (t, J = 8.0 Hz, 2H), 6.71−6.75 (m, 2H), 6.15 (d, J = 7.6 Hz, 2H), 2.45 (s, 6H). Anal. Calcd for $C_{31}H_{22}IrF_3N_4O_3S_3$: C, 44.12; H, 2.63; N, 6.64. Found: C, 43.75; H, 2.73; N, 6.35. ESI-MS: m/z 695.1 ($[M - OTf]^+$).

X-ray Structure Determinations. A single crystal of complex $[Ir(bt)_2(CH_3CN)_2]OTf$ (**Ir-3**) was mounted on a glass fiber and transferred to a Bruker SMART CCD area detector. Crystallographic measurement was carried out using a Bruker SMART CCD diffractometer, σ scans, and graphite-monochromated Mo Kα radiation (λ = 0.71073 Å) at room temperature. The structure was solved by direct methods and refined by full-matrix least-squares on F^2 using the program SHELXS-97.[12] All non-hydrogen atoms were refined anisotropically. Hydrogen atoms were calculated in ideal geometries. For the full-matrix least-squares refinements [$I > 2\sigma(I)$], the unweighted and weighted agreement factors of R1 = $\Sigma(F_o - F_c)/\Sigma F_o$ and wR2 = $[\Sigma\omega(F_o^2 - F_c^2)^2/\Sigma\omega F_o^4]^{1/2}$ were used. The CCDC reference number for $[Ir(bt)_2(CH_3CN)_2]OTf$ is 764139.

Mercury(II) Titration and Selectivity Experiments. A stock solution of Hg(II) ($Hg(ClO_4)_2 \cdot 3H_2O$) was prepared in deionized water, and other stock solutions of the metal ions Ag^+, Cd^{2+}, Co^{2+}, Cr^{3+}, Cu^+, Fe^{2+}, Mg^{2+}, Ni^{2+}, Pb^{2+}, Zn^{2+}, K^+, and Na^+ (1 mM) were also prepared in deionized water. A stock solution of **Ir-1** (1 mM) was prepared in CH_3CN and then diluted to 20 μM with CH_3CN for titration and selectivity experiments. Titration experiments were performed by placing 2 mL of a solution of **Ir-1** (20 μM) in a quartz cuvette of 1 cm optical path length and then adding the Hg(II) stock solution incrementally through a micropipet. Test samples for selective optical response experiments were prepared by adding appropriate amounts of metal ion stock solutions to 2 mL of a solution of **Ir-1** (20 μM). All test solutions were stirred for 5 min and then tested by UV−vis absorption and fluorescence spectrometers. For fluorescence measurements, excitation was provided at 365 nm and emission was collected from 450 to 750 nm.

Cell Culture. The KB and HeLa cell lines were provided by the Institute of Biochemistry and Cell Biology, Chinese Academy of Sciences. The KB and HeLa cells were grown in RPMI 1640 (Roswell Park Memorial Institute's Medium) supplemented with 10% FBS (Fetal Bovine Serum) at 37 °C and 5% CO_2. Cells were plated on 18 mm glass coverslips and allowed to adhere for 24 h.

Confocal Luminescence Imaging. A stock solution of **Ir-1** (1 mM) was prepared in dimethyl sulfoxide (DMSO) and then diluted

dx.doi.org/10.1021/ic102082k |Inorg. Chem. 2011, 50, 7412–7420

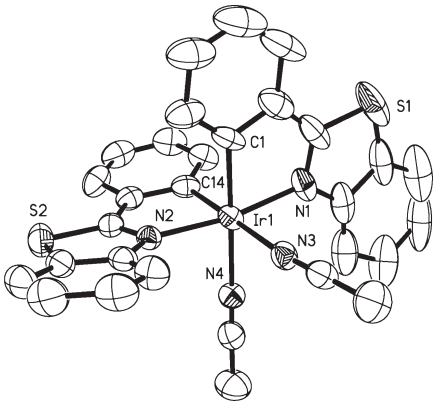

Figure 1. ORTEP diagram of **Ir-3**. Hydrogen atoms and OTf anion were omitted for clarity.

to 10 or 2 μM with phosphate-buffered saline (PBS) for imaging experiments. Confocal luminescence imaging of cells was performed with on an OLYMPUS FV1000 IX8 confocal fluorescence microscope equipped with a 60× oil-immersion objective lens, excitation at 405 nm was carried out with a semiconductor laser, and emission was collected at 515 ± 15 and 560 ± 10 nm.

Theoretical Calculations. Geometric and energy optimizations were performed with the Gaussian 03 program based on the density functional theory (DFT) method.[13] The Becke's three-parameter hybrid functional with the Lee−Yang−Parr correlation functional (B3LYP) was employed for all calculations. The LANL2DZ basis set was used to treat the iridium atom, whereas the 6-31G* basis set was used to treat all other atoms.

RESULTS AND DISCUSSION

Crystal Structure of Ir-3. The single crystal of **Ir-3** was obtained from the mixed solution of CH_2Cl_2 and ether. Figure 1 shows the ORTEP view of **Ir-3**. The crystallographic refinement parameters of **Ir-3** are summarized in Table 1, and the selected bond distances (Angstroms) and angles (degrees) are listed in Table S1 (see Supporting Information).

As shown in Figure 1, the iridium(III) center in **Ir-3** adopts a distorted octahedral coordination geometry with cis-metalated carbons atoms and trans nitrogen atoms, similar to what has been revealed by previous structural studies on mononuclear species containing the C^N cyclometalated ligands.[14] Moreover, the Ir−C (~2.04 Å) and Ir−N (C^N) (~2.06 Å) distances are similar to those reported for other iridium(III) complexes.[14] However, the Ir−N (CH_3CN) distances (2.142(7) and 2.161(7) Å) are longer than the corresponding Ir−N (bt) distances (2.061(5) and 2.064(4) Å) because of their trans influence. In addition, the relatively wide bite angle (87.39°) of N_3−Ir−N_4 may be attributed to the small size of CH_3CN.

Photophysical Properties. The electronic absorption and emission spectra of **Ir-1**, **Ir-2**, and **Ir-3** in CH_2Cl_2 and CH_3CN solutions at room temperature are shown in Figure 2, and the corresponding data are listed in Table 2. With reference to previous photophysical studies on related iridium(III) systems,[15] all complexes have intense absorption bands in the ultraviolet region ca. 260−340 nm, with an extinction coefficient ε of ~10^5 dm^3 mol^{-1} cm^{-1}, which are assigned to spin-allowed singlet intraligand (^{1}LC) transitions ($\pi \rightarrow \pi^*$) (bt and bpy). The weak bands at 350−500 nm with ε of ~10^3 dm^3 mol^{-1} cm^{-1} have

Table 1. Crystallographic Data for Ir-3

	Ir-3 $[Ir(bt)_2(CH_3CN)_2]OTf$
empirical formula	$C_{31}H_{22}F_3IrN_4O_3S_3$
cryst syst	monoclinic
space group	$P2(1)/c$
crystal size (mm)	0.18 × 0.16 × 0.15
a, Å	13.054(3)
b, Å	13.683(3)
c, Å	17.743(4)
α, deg	90
β, deg	91.47(3)
γ, deg	90
V, Å^3	3168.0(11)
Z	4
calcd density, g/cm^3	1.769
μ, mm^{-1}	4.469
F(000)	1648
final R indices [$I > 2\sigma(I)$]	0.0364
wR2 [$I > 2\sigma(I)$]	0.0810
R1 (all data)	0.0668
wR2 (all data)	0.0930
GOF on F^2	0.981

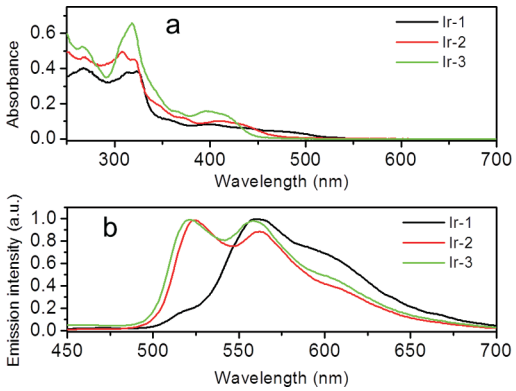

Figure 2. Absorption (a) and emission spectra (b) of **Ir-1**, **Ir-2**, and **Ir-3** in CH_3CN solution with a concentration of 10 μM, λ_{ex} = 365 nm.

been assigned to the mixed singlet and triplet metal-to-ligand charge-transfer (MLCT) transition (dπ(Ir) → π^*(bpy)) and intraligand (LC_{bt}) transitions.

In CH_3CN solution, **Ir-1** displays a structured emission band with a maximum at a wavelength of 563 nm and a shoulder at 603 nm. With reference to quinine sulfate as a standard in an air-equilibrated solution, the quantum efficiencies (Φ_{em}) of **Ir-1** and **Ir-2** in CH_3CN solution were measured to be 0.016 and 0.031, respectively. For the cationic iridium(III) complex **Ir-2** containing a diimine ligand, the emission commonly comes from a mixed excited state containing ^{3}MLCT (dπ(Ir) → π^*_{bpy}) and ^{3}LLCT ($\pi_{bt} \rightarrow \pi^*_{bpy}$) transitions. However, for the neutral complex **Ir-1** containing O^O ligand with a higher triplet energy level, the emission comes from a mixed excited state containing ^{3}LC ($\pi_{bt} \rightarrow \pi^*_{bt}$) and ^{3}MLCT (d$\pi$(Ir) → π^*_{bt}) transitions.[16]

Optical Response of Ir-1 to Hg(II). Recently, fluorescent chemosensors for mercury ions have attracted increasing attention, because mercury is a dangerous and widespread global

dx.doi.org/10.1021/ic102082k |Inorg. Chem. 2011, 50, 7412–7420

Table 2. Photophysical Data of Complexes Ir-1, Ir-2, and Ir-3

complexes	solvent	λ_{abs}/nm (ε/dm^3 mol^{-1} cm^{-1})	$\lambda_{PL,max}$(nm)	Φ_{em}
Ir-1	CH_2Cl_2	266 (34 673), 324 (30 199), 435 (5754)	557, 590sh	
	CH_3CN	269 (33 831), 323 (30 597), 438 (5577)	563, 603sh	0.016
Ir-2	CH_2Cl_2	274 (33 884), 310 (28 840), 412 (6309)	525, 561sh	
	CH_3CN	270 (31 735), 309 (28 953), 409 (6882)	524, 560sh	0.031
Ir-3	CH_2Cl_2	268 (15 135), 322 (19 054), 400 (5011)	516, 548sh	
	CH_3CN	266 (14 876), 318 (19 354), 396 (4851)	520, 560sh	0.008

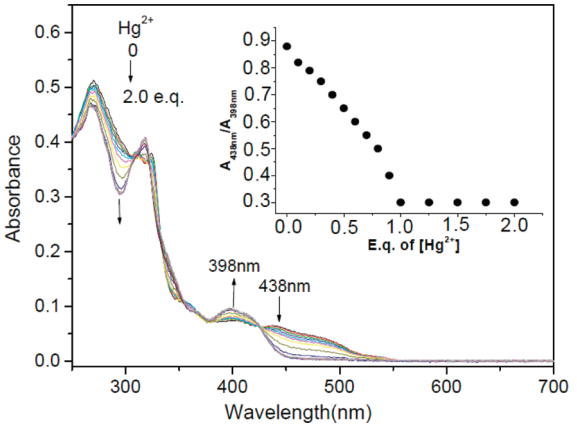

Figure 3. Changes in the UV−vis absorption spectra of **Ir-1** (20 μM) in CH_3CN solution with various amounts of Hg(II) ions (0−40 μM). (Inset) Titration curve of the absorbance ratio at 438 nm to 398 nm for **Ir-1** upon addition of Hg(II) ions.

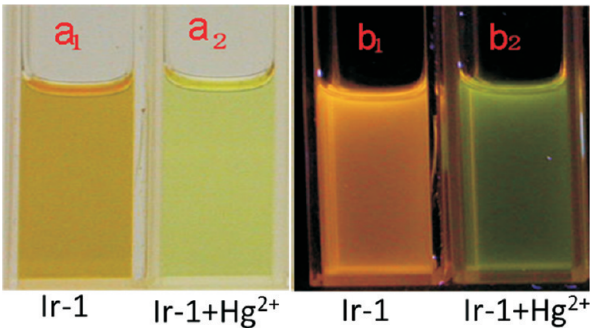

Figure 4. Solution (a) and luminescence (b) color photographs of **Ir-1** (40 μM in CH_3CN solution) before (a_1 and b_1) and after (a_2 and b_2) addition of 1 equiv of Hg(II).

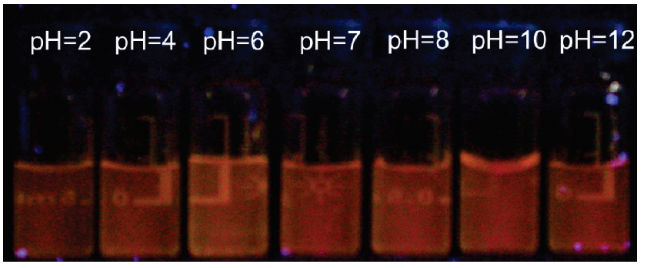

Figure 5. Luminescent photographs of **Ir-1** at different pH values.

pollutant and causes serious environmental and health problems.[17] The responses of **Ir-1**, **Ir-2**, and **Ir-3** to Hg(II) were investigated through titration in UV−vis absorption, phosphorescence emission, and electrochemical titration measurements. No significant changes in the absorption and phosphorescence emissions were observed for **Ir-2** or **Ir-3** (Figures S1−S4 in the Supporting Information). However, **Ir-1** proved to be able to specifically sense Hg(II), as manifested in an evident optical change.

a. UV−vis Absorption Spectroscopy. Figure 3 shows the absorption changes of **Ir-1** as a function of Hg(II) concentration in CH_3CN solution. Upon addition of Hg(II) to a solution of **Ir-1**, the absorption band at 438 nm progressively disappears while a new band appears at 398 nm. The color of the solution changes from yellow to green (Figure 4), indicating that **Ir-1** can serve as a sensitive indicator for Hg(II). The stoichiometry of **Ir-1** is given by the variation of $A_{438\ nm}/A_{398\ nm}$ with respect to the number of equivalents of Hg(II) added. Effectively, A_{438nm}/A_{398nm} decreases continuously until addition of 1 equiv of Hg(II). Further addition of Hg(II) induces only very minor changes in A_{438nm}/A_{398nm} (Figure 3, inset), indicating that **Ir-1** forms a 1:1 complex with Hg(II). The binding constant (K) calculated from absorption titration data is 9.3×10^4 M^{-1}. More importantly, the binding process is fairly fast and we could observe a distinct color change within 2 min. Therefore, **Ir-1** could be potentially used for real-time tracking of Hg(II) in organisms.

b. Luminescent Properties of Ir-1 at Different pH Values. The pH dependence of the luminescent emission of **Ir-1** was investigated. As shown in Figure 5, **Ir-1** exhibits the same emission color (yellow) and intensity at various pH values. Similar phenomena were also observed for **Ir-2** and **Ir-3** (Figure S5 in the Supporting Information). Furthermore, as shown in Figure S6 in the Supporting Information, the emission integral counts of **Ir-1** (10 μM) at different pH values could be calculated to be 7.05×10^6, 6.96×10^6, 6.78×10^6, 6.75×10^6, 7.17×10^6, 7.01×10^6, and 7.24×10^6, corresponding to the pH range from 2 to 12. The average value of emission integral counts at different pH values is 7.05×10^6, and the error of emission integral counts is 0.14×10^6. These facts revealed that **Ir-1** is stable within the pH range from 2 to 12, and its response ability toward Hg(II) is almost invariable. Therefore, complex **Ir-1** can be used to detect Hg(II) without pH interference.

c. Luminescent Spectroscopy. It is well known that luminescent emission spectroscopy is more sensitive toward small changes that affect the electronic properties of molecular receptors. Hence, the response of **Ir-1** to Hg(II) was further investigated by a photoluminescence technique. Upon addition of 1 equiv of Hg(II), the emission band of **Ir-1** exhibited a blue shift of ~40 nm (Figure 6), corresponding to an evident change in emission color from yellow to green (Figure 4). Hence, **Ir-1** shows efficient colorimetric sensing of Hg(II). As determined by

dx.doi.org/10.1021/ic102082k |*Inorg. Chem.* 2011, 50, 7412–7420

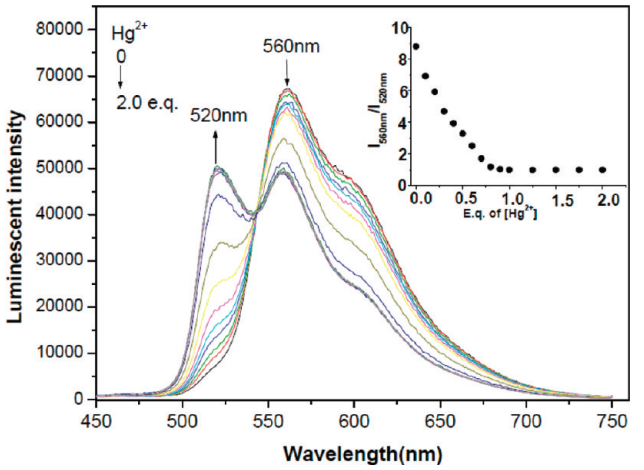

Figure 6. Changes in the luminescence spectra of **Ir-1** (20 μM) in air-equilibrated CH_3CN solution with various amounts of Hg(II) (0−40 μM). (Inset) Titration curve of **Ir-1** with Hg(II).

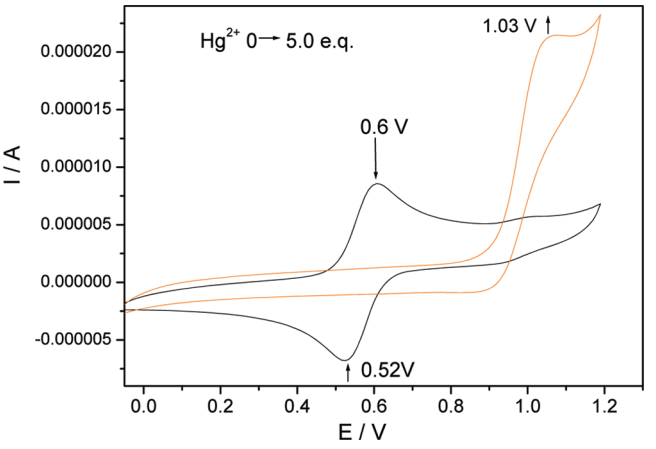

Figure 7. Cyclic voltammograms of **Ir-1** (50 μM) in CH_3CN solution in the absence and presence of 5 equiv of Hg(II) ions.

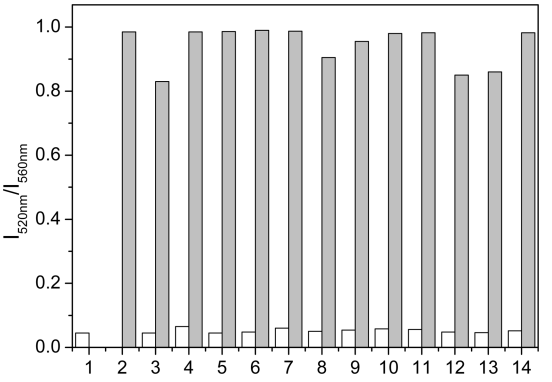

Figure 8. Luminescent response of **Ir-1** (20 μM) in the presence of various metal cations (1 equiv) in CH_3CN solutions. Bars represent the ratio ($I_{520\ nm}/I_{560\ nm}$) of emission intensity at 520 and 560 nm. White bars represent addition of 1-fold various metal cations to a 20 μM solution of **Ir-1**. Solid bars represent the $I_{520\ nm}/I_{560\ nm}$ ratio after addition of Hg(II) (20 μM): (1) without metal cation; (2) Hg^{2+}; (3) Ag^{+}; (4) Cd^{2+}; (5) Co^{2+}; (6) Cr^{3+}; (7) Cu^{+}; (8) Fe^{2+}; (9) Mg^{2+}; (10) Ni^{2+}; (11) Pb^{2+}; (12) Zn^{2+}; (13) K^{+}; (14) Na^{+}.

variations in the luminescence response of **Ir-1** in the presence of various amounts of Hg(II), the stoichiometry of the complex formed between **Ir-1** and Hg(II) is 1:1, which is consistent with the result obtained from the UV−vis absorption spectra. Moreover, in a control experiment, the response of ligand 2-phenylbenzothiazole to Hg(II) was also investigated by absorption and emission spectroscopies. It can be seen from the Figure S7 (see Supporting Information) that no significant changes in absorption and phosphorescence emission were observed for ligand Hbt in CH_3CN solution before and after addition of 2 equiv of Hg(II), which are different from complex **Ir-1**. These observations indicate that **Ir-1** could serve as a "naked eye" indicator for Hg(II) ions.

Electrochemical Studies. Furthermore, the electrochemical response of **Ir-1** to Hg(II) was studied by cyclic voltammetry (CV). In the absence of Hg(II), **Ir-1** shows a quasi-reversible oxidation wave at 0.60 V, which can be assigned to the metal-centered Ir^{III}/Ir^{IV} and cyclometalated ligand oxidation processes.[18] A significant modification in the cyclic voltammetry was observed upon addition of increasing amounts of Hg(II) to a solution of **Ir-1** (Figure 7). The intensity of the oxidation wave at 0.60 V decreased and a new reversible oxidation wave at 1.03 V appeared with the progressive addition of Hg(II). However, the reduction potential of **Ir-1** was hardly changed with various amounts of Hg(II) ions (Figure S8 in the Supporting Information). Moreover, a control experiment about the effect of Hg(II) on the electrochemical signal of ligand Hbt was conducted. As shown in Figure S9 in the Supporting Information, ligand Hbt has a quasi-reversible oxidation wave at 1.67 V. Some changes in the cyclic voltammetry were observed upon addition of excess amounts of Hg(II) to a solution of Hbt, that is, the oxidation wave was shifted positively. Hence, the new reversible oxidation wave at 1.03 V with addition of Hg(II) should be assigned to the metal-centered Ir^{III}/Ir^{IV} and cyclometalated ligand oxidation processes of new complex $[Ir(bt)_2(CH_3CN)_2]^+$ rather than oxidation of Hg(II)−Hbt complex.

Selective Optical Response of Ir-1 to Various Metal Ions. For an excellent chemosensor, high selectivity is a matter of necessity. The selectivity of **Ir-1** for Hg(II) over other cations was evaluated by examination of the emission spectra. In light of the obvious blue shift of the emission spectra for **Ir-1** upon addition of Hg(II), we investigated the selective response of **Ir-1** to various metal ions by using the ratio of the phosphorescent emission intensity at 560 and 520 nm (I_{560nm}/I_{520nm}) as the output signal. To verify a specific response to Hg(II), variations of the luminescence spectra of **Ir-1** caused by other related heavy, transition, and main group metal ions were recorded. As shown in Figure 8 and Figure S10 (in the Supporting Information), only addition of Hg(II) resulted in a prominent luminescence change, whereas addition of 1 equiv of other competitive cations (such as Ag^{+}, Cd^{2+}, Co^{2+}, Cr^{3+}, Cu^{+}, Fe^{2+}, Mg^{2+}, Ni^{2+}, Pb^{2+}, Zn^{2+}, K^{+}, and Na^{+}) caused only slight luminescent changes. Moreover, a competition experiment was done to further explore the utility of **Ir-1** as an ion-selective probe for Hg(II). The coexistent metal cations had a negligible interfering effect on the luminescent blue shift of **Ir-1** upon addition of Hg(II) (Figure S11 in the Supporting Information). All results indicate that the selectivity of **Ir-1** for Hg(II) over other cations is remarkably high.

Furthermore, the selectivity of **Ir-1** for Hg(II) over other cations was also evaluated by examination of the absorption spectra (Figure S12 in the Supporting Information). Herein, the ratio of the absorbance intensity at 438 and 398 nm (A_{438nm}/A_{398nm})

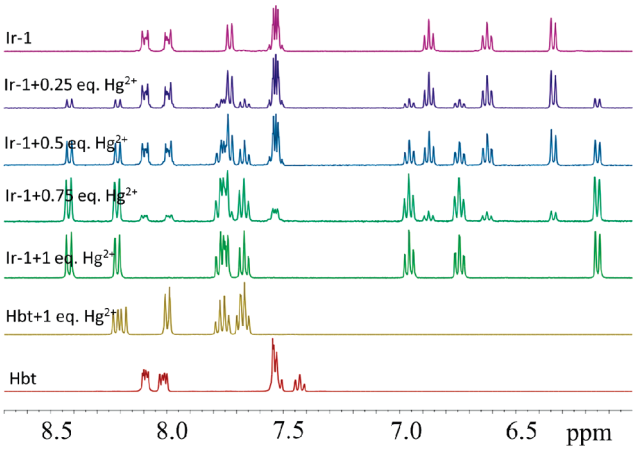

Figure 9. Partial ^{1}H NMR spectral changes of **Ir-1** in CD_3CN in the presence of Hg (II) (0−1 equiv).

was used as the output signal. Due to the low affinity with **Ir-1**, other metal ions (such as Ag^+, Cd^{2+}, Co^{2+}, Cr^{3+}, Cu^+, Fe^{2+}, Mg^{2+}, Ni^{2+}, Pb^{2+}, Zn^{2+}, K^+, and Na^+) showed hardly any change in A_{438nm}/A_{398nm}. However, addition of Hg(II) resulted in a prominent absorption change. These facts indicate that **Ir-1** could be used as a highly selective and ratiometric sensor for Hg(II).

Mechanism of Hg(II) Sensing by Ir-1. In terms of Pearson's hard−soft acid−base theory,[19] Hg(II) is a soft ion (soft acid) and can interact preferentially with sulfur (a soft base). Palomares and co-workers reported that the interaction of Hg(II) with the sulfur atoms in ruthenium complexes induces a color change.[20] We can deduce that the variations in the optical-electrochemical properties of **Ir-1** are due to coordination of Hg(II) by the lone-pair electrons on the sulfur atom of the cyclometalated ligand 2-phenylbenzothiazole (bt). Herein, to seek further detailed information on the binding mechanism, ^{1}H NMR spectroscopic titration experiments of complex **Ir-1** with different equivalents of Hg(II) ion were conducted. Upon addition of Hg(II) ion, a variation in the ^{1}H NMR spectra of **Ir-1**, especially in the cyclometalated ligand bt moiety (see Figure 9), was observed. However, no ^{1}H NMR characteristic peaks at δ = 8.09, 8.07, 7.53, and 7.43 ppm that correspond to free Hbt appeared upon addition of various amounts of Hg(II), indicating that the ligand bt still bound with iridium(III). Interestingly, the characteristic peaks of free Hacac at 2.01 ppm appeared for **Ir-1** in the presence of 1.0 equiv of Hg(II) (Figure S13 in the Supporting Information), suggesting that ligand acac was removed from complex **Ir-1**. Hence, we can deduce that rupture of Ir−O coordinated bonds occurs and free acac ligand is released from **Ir-1** after addition of Hg(II). Furthermore, the ^{1}H NMR peaks of $[Ir(bt)_2(CH_3CN)_2]^+$ can be found in the spectrum of the mixture of **Ir-1** with Hg(II) (Figure S14 in the Supporting Information). Therefore, we tentatively summarize the sensing mechanism of **Ir-1** with Hg(II) as follows (see Scheme 2): the sulfur atoms (soft base) on the bt ligand bind with Hg(II) (soft acid) according to Pearson's soft−hard acid−base theory, which induces fast decomposition of **Ir-1** with departure of acac from the complex to form a new complex $[Ir(bt)_2(CH_3CN)_2]^+$. Such a process results in the evident changes of absorption, emission, and electrochemical properties.

The sensing responses of complexes **Ir-2** and **Ir-3** to Hg(II) were very weak, which is different from those of **Ir-1**. In order to clarify such difference, the charge distributions of these complexes

Scheme 2. Illustration of the Sensing Mechanism

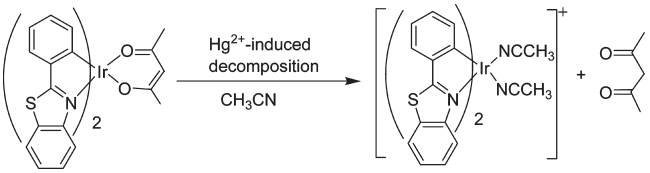

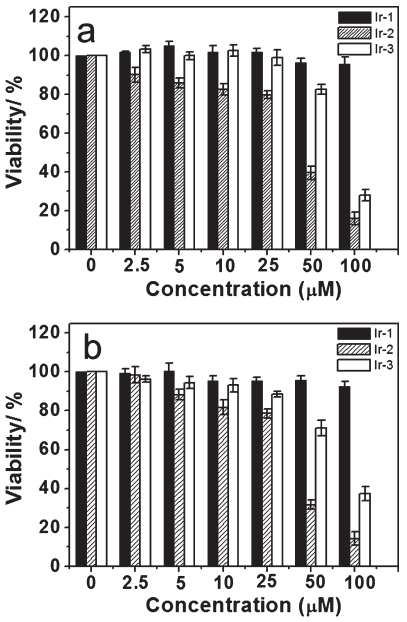

Figure 10. Cell viability values (%) estimated by MTT proliferation test versus incubation concentrations of **Ir-1**, **Ir-2**, and **Ir-3**. KB (a) and HeLa (b) cells were cultured in the presence of 5−100 μM complexes at 37 °C for 24 h.

were investigated through DFT calculations. Surface charge analysis based on DFT calculations indicated that the charge on the sulfur atom of **Ir-1** (the electron cloud density 0.247) is more negative than those of **Ir-2** (the electron cloud density 0.310) and **Ir-3** (the electron cloud density 0.292). Thus, **Ir-1** combines with Hg(II) to form a coordinated complex more easily, whereas **Ir-2** and **Ir-3** exhibit weaker coordination ability toward Hg(II). In addition, **Ir-2** and **Ir-3** are cationic, making coordination with Hg(II) more difficult.

Cytotoxicity of Ir-1. We selected two cell lines (KB and HeLa cells) for investigation of the toxicity about three Ir complexes, and the toxicity data are shown in Figure 10. Upon incubation with **Ir-1** (10 μM) for 24 h, only less than 5% of the KB and HeLa cells died. When the concentration of **Ir-1** was increased to 25 and 100 μM, the cell viability still remains above 90%. For the other two complexes **Ir-2** and **Ir-3**, their cytotoxicity is higher than that of **Ir-1**, especially at high concentration (>50 μM). However, at the concentration (10 μM) of the cell imaging experiment, the cell viability of these two complexes for both KB and HeLa remains above 80%, even with an incubation time of 24 h. These three complexes show relatively low cytotoxicity in the cell imaging experiment (concentration of 10 μM and incubation time of 15 min). In particular, complex **Ir-1** exhibits the lowest cytotoxicity both at low and at high concentration and will not kill the cell being probed.

dx.doi.org/10.1021/ic102082k |*Inorg. Chem.* 2011, 50, 7412–7420

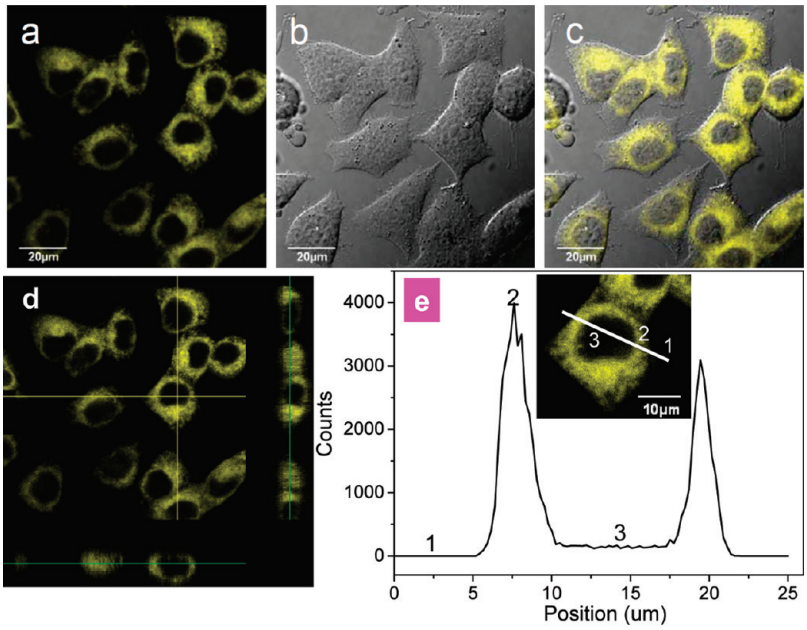

Figure 11. Confocal luminescence (a), bright-field (b), and overlay (c) images of living KB cells incubated with **Ir-1** (10 μM) in PBS for 15 min at 37 °C (λ_{ex} = 405 nm). (d) Overlap *Z*-scan confocal image of the living KB cells incubated with **Ir-1** (10 μM). (e) Luminescence intensity profile and luminescence image (across the line) of KB cells.

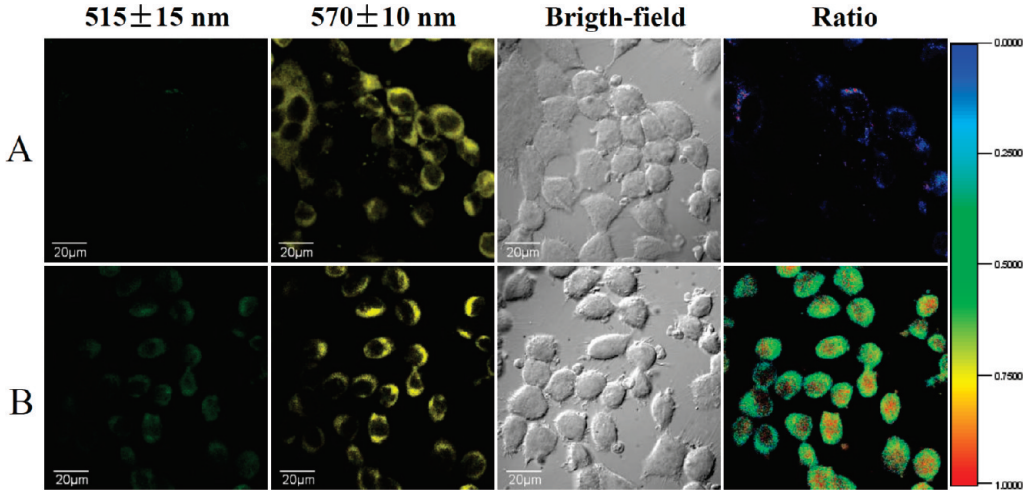

Figure 12. Ratiometric phosphorescence images of **Ir-1**-incubated KB cells treated without or with Hg(II). (A) KB cells incubated with **Ir-1** for 15 min. (B) KB cells incubated with **Ir-1** (10 μM) for 15 min and then further treated with 100 μM Hg(II) for 1 h. Emission was collected by the green channel (515 ± 15 nm) and yellow channel (570 ± 10 nm) (λ_{ex} = 405 nm). Ratio of emission intensity at 515 ± 15 to 570 ± 10 nm is also shown.

Luminescence Bioimaging of Hg(II) in Living Cells Using Ir-1. In contrast to conventional luminescence-enhanced detection, ratiometric measurement allows simultaneous recording of two emission intensities at different wavelengths in the presence and absence of analytes and thus provides built-in correction for environmental effects.[21] As described above, addition of Hg(II) into an **Ir-1** solution induced a blue shift of approximately 40 nm in the emission spectrum. Therefore, **Ir-1** has the potential to serve as a luminescent probe in ratiometric bioimaging. The applicability of **Ir-1** in the ratiometric monitoring of intracellular Hg(II) was investigated by confocal luminescence microscopy. For this, optical windows at 515 ± 15 (green channel) and 570 ± 10 nm (yellow channel) were chosen as the two signal outputs. For adequate interaction between **Ir-1** and intracellular Hg(II), the reaction was allowed to proceed at 37 °C for 1 h. As shown in Figure 11, intense emission was observed within the KB cells incubated with 10 μM **Ir-1** in PBS for 15 min at 37 °C. Overlay of confocal luminescence and bright-field images demonstrated that the luminescence was evident in the cytoplasm over the nucleus and membrane (Figure 11c), which was further confirmed by *Z*-scan confocal microscopy (Figure 11d and movie in the Supporting Information) and quantization analysis of luminescence intensity. As shown in Figure 11e, further quantization by line plots (inset) revealed that the signal ratio (I_2/I_3) between the cytoplasm (region 2) and nucleus (region 3) reached 16, implying weak nuclear uptake of **Ir-1**. The bioimaging results

dx.doi.org/10.1021/ic102082k |*Inorg. Chem.* 2011, 50, 7412–7420

indicated that the neutral complex **Ir-1** had good cell membrane permeability and entered the living cells easily. This is the first case of a neutral iridium(III) complex as a luminescent probe for cell imaging application, although approximately 50 cationic iridium(III) complexes have been used as bioimaging probes.[7−10]

Concerning the ratiometric bioimaging, KB cells incubated with 10 μM **Ir-1** for 15 min showed an emission ratio I_{515nm}/I_{570nm} of ~0.1 between the green luminescence channel (515 ± 15 nm) and the yellow luminescence channel (570 ± 10 nm), as shown in Figure 12A. The **Ir-1**-treated cells were then exposed to 100 μM Hg(II) for 1 h at 37 °C. The phosphorescence intensity of the green channel increased, while that of the yellow channel decreased slightly, and the ratio of luminescence intensities at 515 ± 15 and 570 ± 10 nm was increased to >0.6 (Figure 12B). Furthermore, **Ir-1** can sense the change of Hg(II) in living cell incubated with 10 μM Hg(II) (Figure S15 in Supporting Information). KB cells incubated with 2 μM **Ir-1** for 30 min showed an emission ratio I_{515nm}/I_{570nm} of <0.2. The **Ir-1**-incubated cells were then exposed to 10 μM Hg(II) for 8 h at 37 °C. The phosphorescence intensity of the green luminescence channel increased, and the emission ratio I_{515nm}/I_{570nm} was increased to ≥0.6. These data suggest that **Ir-1** could still be used for monitoring changes in a low concentration of Hg(II).

CONCLUSIONS

In summary, we demonstrated the internalization of a neutral iridium(III) complex **Ir-1** into living cells and further selective detection of Hg(II) in cell samples by ratiometric measurement. Compared to two cationic complexes **Ir-2** and **Ir-3**, **Ir-1** specifically responds to Hg(II) with a noticeable change in phosphorescent emission color from yellow to green. The interaction between Hg(II) and the sulfur atom of the C^N cyclometalated ligand is responsible for the significant variations in the optical and electrochemical signals. Importantly, cell imaging experiments have demonstrated that **Ir-1** is membrane permeable and can readily reveal changes in intracellular Hg(II) concentration in a ratiometric way. To our knowledge, this is the first report of a neutral iridium complex entering living cells and realizing ratiometric bioimaging of Hg(II). The result described herein may well be of interest to others working in the areas of phosphorescent heavy metal complexes, bioimaging, and luminescent molecular probes.

ASSOCIATED CONTENT

Supporting Information. Selected bond distances and angles for **Ir-3**, changes in the absorption and luminescence spectra of **Ir-2** in CH_3CN solution with various amounts of Hg(II), changes in the luminescence spectra of **Ir-3** (5 μM) in air-equilibrated CH_3CN solution with various amounts of Hg(II) ions (0−250 μM), luminescent photographs of **Ir-2** and **Ir-3** at different pH values, luminescent spectra and luminescent integral counts of **Ir-1** (10 μM) at different pH values, absorption and emission spectra of ligand 2-phenylbenzothiazole (Hbt) in CH_3CN solution without and with 2 equiv of Hg(II) ions, changes in the reduction potential of **Ir-1** with various amounts of Hg(II), cyclic voltammograms of Hbt (0.5 mM) in CH_3CN solution in the absence and presence of various amounts of Hg(II) ions (0−2.5 mM), response of luminescent spectra of **Ir-1** (5 μM) in CH_3CN solution to different competition ions, absorption response of **Ir-1** in the presence of various metal cations, partial ^{1}H NMR spectral changes of **Ir-1** in CD_3CN in the presence of mercury(II) (0−1 equiv), partial ^{1}H NMR spectra of **Ir-1** with mercury(II) and **Ir-3** in CD_3CN, ratiometric phosphorescence images of **Ir-1**-incubated KB cells treated without or with Hg(II) (10 μM), and cell imaging for $[Ir(bt)_2(bpy)]PF_6$. This material is available free of charge via the Internet at http://pubs.acs.org.

AUTHOR INFORMATION

Corresponding Author

*Phone: 86-21-55664185. Fax: 86-21-55664621. E-mail: fyli@fudan.edu.cn (F.Y.L.), iamqzhao@njupt.edu.cn (Q.Z.).

ACKNOWLEDGMENT

The authors thank the National Natural Science Funds for Distinguished Young Scholars (20825101), National Natural Science Foundation of China (50803028 and 20804019), Shanghai Sci. Tech. Comm. (1052 nm03400), Shanghai Leading Academic Discipline Project (B108), IRT0911, and Scientific and Technological Activities for Returned Personnel in Nanjing City (NJ209001) for financial support.

REFERENCES

(1) (a) Chi, Y.; Chou, P. T. *Chem. Soc. Rev.* **2010**, *39*, 638. (b) Lo, K. K. W.; Louie, M. W.; Zhang, K. Y. *Coord. Chem. Rev.* **2010**, *254*, 2603. (c) Chen, Z. Q.; Bian, Z. Q.; Huang, C. H. *Adv. Mater.* **2010**, *22*, 1534. (d) Zhao, Q.; Liu, S. J.; Huang, W. *Macromol. Rapid Commun.* **2010**, *31*, 794. (e) Wong, W. Y.; Ho, C. L. *Coord. Chem. Rev.* **2009**, *253*, 1709. (f) You, Y.; Park, S. Y. *Dalton Trans.* **2009**, *8*, 1267. (g) Ulbricht, C.; Beyer, B.; Friebe, C.; Winter, A.; Schubert, U. S. *Adv. Mater.* **2009**, *21*, 4418. (h) Thompson, M. E. *MRS Bull.* **2007**, *32*, 694. (i) Liu, S. J.; Zhao, Q.; Fan, Q. L.; Huang, W. *Eur. J. Inorg. Chem.* **2008**, 2177. (j) Liu, S. J.; Zhao, Q.; Huang, W. *Adv. Polym. Sci.* **2008**, *212*, 125.

(2) (a) Wu, C.; Chen, H. F.; Wong, K. T.; Thompson, M. E. *J. Am. Chem. Soc.* **2010**, *132*, 3133. (b) Mauro, M.; Schuermann, K. C.; Prétôt, R.; Hafner, A.; Mercandelli, P.; Sironi, A.; De Cola, L. *Angew. Chem., Int. Ed.* **2010**, *49*, 1222. (c) Chiu, Y. C.; Hung, J. Y.; Chi, Y.; Chen, C. C.; Chang, C. H.; Wu, C. C.; Cheng, Y. M.; Yu, Y. C.; Lee, G. H.; Chou, P. T. *Adv. Mater.* **2009**, *21*, 2221. (d) Tan, W. J.; Zhang, Q.; Zhang, J. J.; Tian, H. *Org. Lett.* **2009**, *11*, 161. (e) He, L.; Qiao, J.; Duan, L.; Dong, G. F.; Zhang, D. Q.; Wang, L. D.; Qiu, Y. *Adv. Funct. Mater.* **2009**, *19*, 1. (f) Lee, S. J.; Park, K. M.; Yang, K.; Kang, Y. *Inorg. Chem.* **2009**, *48*, 1030.

(3) (a) Botchway, S. W.; Charnley, M.; Haycock, J. W.; Parker, A. W.; Rochester, D. L.; Weinstein, J. A.; Gareth Williams, J. A. *Proc. Natl. Acad. Sci. U.S.A.* **2008**, *105*, 16071. (b) Murphy, L.; Congreve, A.; Palsson, L. O.; Gareth Williams, J. A. *Chem. Commun.* **2010**, *46*, 8743.

(4) Zhao, Q.; Li, F. Y.; Huang, C. H. *Chem. Soc. Rev.* **2010**, *39*, 3007.

(5) (a) Ho, M. L.; Hwang, F. M.; Chen, P. N.; Hu, Y. H.; Cheng, Y. M.; Chen, K. S.; Lee, G. H.; Chi, Y.; Chou, P. T. *Org. Biomol. Chem.* **2006**, *4*, 98. (b) Ho, M. L.; Cheng, Y. M.; Wu, L. C.; Chou, P. T.; Lee, G. H.; Hsu, F. C.; Chi, Y. *Polyhedron* **2007**, *26*, 4886. (c) Schmittel, M.; Lin, H. *Inorg. Chem.* **2007**, *46*, 9139. (d) You, Y.; Park, S. Y. *Adv. Mater.* **2008**, *20*, 3820.

(6) (a) Zhao, Q.; Cao, T. Y.; Li, F. Y.; Li, X. H.; Jing, H.; Yi, T.; Huang, C. H. *Organometallics* **2007**, *26*, 2077. (b) Zhao, Q.; Liu, S. J.; Shi, M.; Li, F. Y.; Jing, H.; Yi, T.; Huang, C. H. *Organometallics* **2007**, *26*, 5922. (c) Chen, H. L.; Zhao, Q.; Wu, Y. B.; Li, F. Y.; Yang, H.; Yi, T.; Huang, C. H. *Inorg. Chem.* **2007**, *46*, 11075. (d) Zhao, Q.; Li, F. Y.; Liu, S. J.; Yu, M. X.; Liu, Z. Q.; Yi, T.; Huang, C. H. *Inorg. Chem.* **2008**, *47*, 9256. (e) Zhao, Q.; Liu, S. J.; Li, F. Y.; Yi, T.; Huang, C. H. *Dalton Trans.* **2008**, *29*, 3836. (f) Xu, W. J.; Liu, S. J.; Zhao, X. Y.; Sun, S.; Cheng, S.; Ma, T. C.; Sun, H. B.; Zhao, Q.; Huang, W. *Chem.—Eur. J.* **2010**, *16*, 7125. (g) Shi, H. F.; Liu, S. J.; Sun, H. B.; Xu, W. J.; An, Z. F.; Chen, J.;

Sun, S.; Lu, X. M.; Zhao, Q.; Huang, W. *Chem.—Eur. J.* **2010**, *16*, 12158. (h) Xu, W. J.; Liu, S. J.; Sun, H. B.; Zhao, X. Y.; Zhao, Q.; Sun, S.; Cheng, S.; Ma, T. C.; Zhou, L. X.; Huang, W. *J. Mater. Chem.* **2011**, *21*, 7572. (j) Liu, Y.; Li, M. Y.; Zhao, Q.; Wu, H. Z.; Huang, K. W.; Li, F. Y. *Inorg. Chem.* 2011, ASAP. doi./10.1021/ic102481x

(7) (a) Lo, K. K. W.; Tsang, K. H. K.; Sze, K. S.; Chung, C. K.; Lee, T. K. M.; Zhang, K. Y.; Hui, W. K.; Li, C. K.; Lau, J. S. Y.; Ng, D. C. M.; Zhu, N. *Coord. Chem. Rev.* **2007**, *251*, 2292. (b) Moreira, V. F.; Greenwood, F. L. T.; Coogan, M. P. *Chem. Commun.* **2010**, *46*, 186. (c) Zhao, Q.; Huang, C. H.; Li, F. Y. *Chem. Soc. Rev.* **2011**, *40*, 2508.

(8) (a) Lo, K. K. W.; Lee, P. K.; Lau, J. S. Y. *Organometallics* **2008**, *27*, 2998. (b) Lau, J. S. Y.; Lee, P. K.; Tsang, K. H. K.; Ng, C. H. C.; Lam, Y. W.; Cheng, S. H.; Lo, K. K. W. *Inorg. Chem.* **2009**, *48*, 708. (c) Zhang, K. Y.; Lo, K. K. W. *Inorg. Chem.* **2009**, *48*, 6011. (d) Zhang, K. Y.; Li, S. P. Y.; Zhu, N. Y.; Or, I. W. S.; Cheung, M. S. H.; Lam, Y. W.; Lo, K. K. W. *Inorg. Chem.* **2010**, *49*, 2530. (e) Leung, S. K.; Kwok, K. Y.; Zhang, K. Y.; Lo, K. K. W. *Inorg. Chem.* **2010**, *49*, 4984. (f) Zhang, K. Y.; Liu, H. W.; Fong, T. T. H.; Chen, X. G.; Lo, K. K. W. *Inorg. Chem.* **2010**, *49*, 5432. (g) Liu, H. W.; Zhang, K. Y.; Law, W. H. T.; Lo, K. K. W. *Organometallics* **2010**, *29*, 3474.

(9) (a) Yu, M. X.; Zhao, Q.; Shi, L. X.; Li, F. Y.; Zhou, Z. G.; Yang, H.; Yi, T.; Huang, C. H. *Chem. Commun.* **2008**, 2115. (b) Zhao, Q.; Yu, M. X.; Shi, L. X.; Liu, S. J.; Li, C. Y.; Shi, M.; Zhou, Z. G.; Huang, C. H.; Li, F. Y. *Organometallics* **2010**, *29*, 1085. (c) Jiang, W. L.; Gao, Y.; Sun, Y.; Ding, F.; Xu, Y.; Bian, Z. Q.; Li, F. Y.; Bian, J.; Huang, C. H. *Inorg. Chem.* **2010**, *49*, 3252. (d) Wu, H. Z.; Yang, T. S.; Zhao, Q.; Zhou, J.; Li, C. Y.; Li, F. Y. *Dalton Trans.* **2011**, *40*, 1969.

(10) Xiong, L. Q.; Zhao, Q.; Chen, H. L.; Wu, Y. B.; Dong, Z. S.; Zhou, Z. G.; Li, F. Y. *Inorg. Chem.* **2010**, *49*, 6402.

(11) Lamansky, S.; Djurovich, P.; Murphy, D.; Abdel-Razzaq, F.; Lee, H. E.; Adachi, C.; Burrows, P. E.; Forrest, S. R.; Thompson, M. E. *J. Am. Chem. Soc.* **2001**, *123*, 4304. (b) Lamansky, S.; Djurovich, P.; Murphy, D.; Abdel-Razzaq, F.; Kwong, R.; Tsyba, I.; Bortz, M.; Mui, B.; Bau, R.; Thompson., M. E. *Inorg. Chem.* **2001**, *40*, 1704.

(12) Sheldrick, G. M. *SHELXTL-Plus VS.1 software Reference Manual*; Bruker AXS Inc.: Madison, WI, 1997.

(13) Frisch, M. J.; Trucks, G. W.; Schlegel, H. B.; Scuseria, G. E.; Robb, M. A.; Cheeseman, J. R.; Montgomery, J. A., Jr.; Vreven, T.; Kudin, K. N.; Burant, J. C.; Millam, J. M.; Iyengar, S. S.; Tomasi, J.; Barone, V.; Mennucci, B.; Cossi, M.; Scalmani, G.; Rega, N.; Petersson, G. A.; Nakatsuji, H.; Hada, M.; Ehara, M.; Toyota, M.; Fukuda, R.; Hasegawa, J.; Ishida, M.; Nakajima, T.; Honda, Y.; Kitao, O.; Nakai, H.; Klene, M.; Li, X.; Knox, J. E.; Hratchian, H. P.; Cross, J. B.; Adamo, C.; Jaramillo, J.; Gomperts, R.; Stratmann, R. E.; Yazyev, O.; Austin, A. J.; Cammi, R.; Pomelli, C.; Ochterski, J. W.; Ayala, P. Y.; Morokuma, K.; Voth, G. A.; Salvador, P.; Dannenberg, J. J.; Zakrzewski, V. G.; Dapprich, S.; Daniels, A. D.; Strain, M. C.; Farkas, O.; Malick, D. K.; Rabuck, A. D.; Raghavachari, K.; Foresman, J. B.; Ortiz, J. V.; Cui, Q.; Baboul, A. G.; Clifford, S.; Cioslowski, J.; Stefanov, B. B.; Liu, G.; Liashenko, A.; Piskorz, P.; Komaromi, I.; Martin, R. L.; Fox, D. J.; Keith, T.; Al-Laham, M. A.; Peng, C. Y.; Nanayakkara, A.; Challacombe, M.; Gill, P. M. W.; Johnson, B.; Chen, W.; Wong, M. W.; Gonzalez, C.; Pople, J. A. *GAUSSIAN 03*, Revision C.02; Gaussian, Inc.: Wallingford, CT, 2004.

(14) Neve, F.; Deda, M. L.; Crispini, A.; Bellusci, A.; Puntoriero, F.; Campagna, S. *Organometallics* **2004**, *23*, 5856.

(15) (a) Sprouse, S.; King, K. A.; Spellane, P. J.; Watts, R. J. *J. Am. Chem. Soc.* **1984**, *106*, 6647. (b) Didier, P.; Ortmans, I.; Kirsch-De Mesmaeker, A.; Watts, R. J. *Inorg. Chem.* **1993**, *32*, 5239. (c) Ortmans, I.; Didier, P.; Kirsch-De Mesmaeker, A. *Inorg. Chem.* **1995**, *34*, 3695. (d) Dixon, I. M.; Collin, J.-P.; Sauvage, J. P.; Flamigni, L.; Encinas, S.; Barigelletti, F. *Chem. Soc. Rev.* **2000**, *29*, 385. (e) Auffrant, A.; Barbieri, A.; Barigelletti, F.; Lacour, J.; Mobian, P.; Collin, J. P.; Sauvage, J. P.; Ventura, B. *Inorg. Chem.* **2007**, *46*, 6911.

(16) Zhao, Q.; Liu, S. J.; Shi, M.; Wang, C. M.; Yu, M. X.; Li, L.; Li, F. Y.; Yi, T.; Huang, C. H. *Inorg. Chem.* **2006**, *45*, 6152.

(17) (a) U.S. EPA, *Regulatory Impact Analysis of the Clean Air Mercury Rule*: EPA-452/R-05-003, 2005. (b) Wu, D. Y.; Huang, W.; Liu, Z. H.; Duan, C. Y.; He, C.; Wu, S.; Wang, D. H. *Inorg. Chem.* **2008**, *47*, 7190. (c) He, G. J.; Zhao, Y. G.; He, C.; Liu, Y.; Duan, C. Y. *Inorg. Chem.* **2008**, *47*, 5169. (d) Zhang, X. L.; Xiao, Y.; Qian, X. H. *Angew. Chem., Int. Ed.* **2008**, *47*, 8025. (e) Yang, H.; Zhou, Z. G.; Huang, K. W.; Yu, M. X.; Li, F. Y.; Yi, T.; Huang, C. H. *Org. Lett.* **2007**, *9*, 4729. (f) Liu, S. J.; Fang, C.; Zhao, Q.; Fan, Q. L.; Huang, W. *Macromol. Rapid Commun.* **2008**, *29*, 1212.

(18) (a) van Diemen, J. H.; Hage, R.; Haasnoot, J. G.; Lempers, H. E. B.; Reedijk, J.; Vos, J. G.; De Cola, L.; Barigelletti, F.; Balzani, V. *Inorg. Chem.* **1992**, *31*, 3518. (b) McDaniel, N. D.; Coughlin, F. J.; Tinker, L. L.; Bernhard, S. *J. Am. Chem. Soc.* **2008**, *130*, 210. (c) Lo, K. K.-W.; Li, C.-K.; Lau, J. S.-Y. *Organometallics* **2005**, *24*, 4594. (d) Lo, K. K. W.; Lau, J. S. Y. *Inorg. Chem.* **2007**, *46*, 700.

(19) Pearson, R. G. *J. Am. Chem. Soc.* **1963**, *85*, 3533.

(20) Coronado, E.; Galan-Mascaros, J. R.; Marti-Gastaldo, C.; Palomares, E. J.; Durrant, R. R.; Vilar, R.; Gratzel, M.; Nazeeruddin, Md. K. *J. Am. Chem. Soc.* **2005**, *127*, 12351.

(21) (a) Maruyama, S.; Kikuchi, K.; Hirano, T.; Urano, Y.; Nagano, T. *J. Am. Chem. Soc.* **2002**, *124*, 1065. (b) Taki, M.; Wolford, J. L.; O'Halloran, T. V. *J. Am. Chem. Soc.* **2004**, *126*, 712. (c) Jares-Erijman, E. A.; Jovin, T. M. *Nat. Biotechnol.* **2003**, *21*, 1387. (d) Sapsford, K. E.; Berti, L.; Medintz, I. L. *Angew. Chem., Int. Ed.* **2006**, *45*, 4562. (e) Liu, B.; Tian, H. *Chem. Commun.* **2005**, 3156. (e) Zhou, Z. G.; Yu, M. X.; Yang, H.; Huang, K. W.; Li, F. Y.; Yi, T.; Huang, C. H. *Chem. Commun.* **2008**, 3387.